




# *Toxoplasma gondii* induces metabolic disturbances in the hippocampus of BALB/c mice

Jun Ma<sup>1</sup> · Jun-Jun He<sup>1</sup> · Meng Wang<sup>1</sup> · Jun-Ling Hou<sup>1</sup> · Hany M. Elsheikha<sup>2</sup> · Xing-Quan Zhu<sup>1,3,4</sup> 

Received: 6 April 2021 / Accepted: 11 June 2021 / Published online: 5 July 2021  
© The Author(s), under exclusive licence to Springer-Verlag GmbH Germany, part of Springer Nature 2021

## Abstract

*Toxoplasma gondii* can cross the blood-brain barrier and infect different regions of the brain including the hippocampus. In the present study, we examined the impact of *Toxoplasma gondii* infection on the metabolism of the hippocampus of female BALB/c mice compared to control mice using ultra-high-performance liquid chromatography-tandem mass spectrometry. Multivariate analysis revealed significant differences between infected and control hippocampi and identified 25, 82, and 105 differential metabolites (DMs) in the infected hippocampi at 7, 14, and 21 days post-infection (dpi), respectively. One DM (sphingosylphosphocholine in the sphingolipid metabolism pathway) and 11 dysregulated pathways were detected at all time points post-infection, suggesting their important roles in the neuropathogenesis of *T. gondii* infection. These pathways were related to neural activity, such as inflammatory mediator regulation of TRP channels, retrograde endocannabinoid signaling, and arachidonic acid metabolism. Weighted correlation network analysis and receiver operating characteristic analysis identified 33 metabolites significantly associated with *T. gondii* infection in the hippocampus, and 30 of these were deemed as potential biomarkers for *T. gondii* infection. This study provides, for the first time, a global view of the metabolic perturbations that occur in the mouse hippocampus during *T. gondii* infection. The potential relevance of the identified metabolites and pathways to the pathogenesis of cognitive impairment and psychiatric disorders are discussed.

**Keywords** *Toxoplasma gondii* · Hippocampus · Metabolomics · Mouse · Infection · Host-pathogen interaction

---

Handling Editor: Una Ryan

---

✉ Hany M. Elsheikha  
hany.elsheikha@nottingham.ac.uk

✉ Xing-Quan Zhu  
xingquanzhu1@hotmail.com

<sup>1</sup> State Key Laboratory of Veterinary Etiological Biology, Key Laboratory of Veterinary Parasitology of Gansu Province, Lanzhou Veterinary Research Institute, [Chinese Academy of Agricultural Sciences, Lanzhou, Gansu Province 730046, People's Republic of China

<sup>2</sup> Faculty of Medicine and Health Sciences, School of Veterinary Medicine and Science, University of Nottingham, Loughborough LE12 5RD, UK

<sup>3</sup> College of Veterinary Medicine, Shanxi Agricultural University, Taigu, Shanxi Province 030801, People's Republic of China

<sup>4</sup> Key Laboratory of Veterinary Public Health of Higher Education of Yunnan Province, College of Veterinary Medicine, Yunnan Agricultural University, Kunming, People's Republic of China

## Introduction

The protozoan *Toxoplasma gondii* is one of the most successful opportunistic pathogens, affecting nearly one-third of the world's human population (Tenter et al. 2000). This parasite can penetrate various biological barriers, such as the blood-brain barrier, and infects different regions of the brain where it causes structural and functional alterations, resulting in encephalopathy, cognitive impairment, and other pathological changes (Marra 2018). The ability of *T. gondii* to modify the behavior or cognitive performance of the host, and its relevance as a risk factor for psychiatric disorders, such as schizophrenia is being increasingly recognized (Elsheikha et al. 2016). *Toxoplasma gondii* infection can also alter the behavior of the murine host to facilitate its own transmission to the definitive feline host (Evans et al. 2014; Ingram et al. 2013).

The exact mechanism linking *T. gondii* infection and psychiatric disorders remains incompletely understood. However, previous studies have shown that *T. gondii* alters gene expression of the infected brains and changes neurotransmitter receptor distribution on neurons in mice (He et al. 2019;

Mendez and Koshy 2017; Zhou et al. 2013). The neuroinflammation associated with *T. gondii* infection can modify the behavior of mice (Boillat et al. 2020). *Toxoplasma gondii* can also alter the metabolic pathways that regulate the neural activity, such as dopamine, tryptophan, and quinolinic acid pathways (Elsheikha et al. 2016) and change the abundances of neurochemical metabolites in the brain, such as phenylalanine and tryptophan (Ma et al. 2020; Ma et al. 2019; Zhou et al. 2015). Patients with psychosis can have alterations in the levels of creatine, glutamate, kynurenine, lactate, N-acetylaspartate, and tryptophan (Li et al. 2018), and metabolic decline can underpin cognitive impairment in Alzheimer's disease (Wilkins and Trushina 2017).

Different parts of the brain perform different biological functions. For example, the cerebral cortex, one of the largest brain tissues, regulates body movement and language comprehension (Bedny et al. 2008; Binder et al. 2005; Huth et al. 2016). The cerebellum controls mood, learning, motor coordination, and food-anticipatory activity (Abdoli and Dalimi 2014; Mendoza et al. 2010; Reeber et al. 2013). The hippocampus plays a role in learning and memory processes and also controls natural defense behavior and emotion processing, such as depression and stress (da Silva and Langoni 2009). A previous study showed an association between the alteration of hippocampal metabolism due to prenatal stress and depressive-like behaviors in rats (Zhang et al. 2019). Mass spectroscopy has been employed to examine the metabolomic signatures of the whole brain, cerebral cortex, cerebellum, spleen, liver, and serum of mice following *T. gondii* infection (Chen et al. 2018; Chen et al. 2017; Ma et al. 2020; Ma et al. 2019; Zhou et al. 2015; Zhou et al. 2016). These studies showed that *T. gondii* infection induced significant alterations of several pathways (e.g., arachidonic acid metabolism and hormone biosynthesis).

Given the aforementioned functions of the hippocampus and the relative preference of *T. gondii* to mouse hippocampus (Berenreiterova et al. 2011), it is possible that metabolic alterations in the hippocampus caused by *T. gondii* infection underpin some of the mechanisms mediating behavioral changes and cognitive deficits (Elsheikha et al. 2016; Evans et al. 2014; Groer et al. 2011; Hsu et al. 2014; Ingram et al. 2013). Therefore, a better understanding of the metabolic perturbation in the hippocampus caused by *T. gondii* infection may reveal important aspects of the parasite neuropathogenesis, as well as processes that underpin infection-related cognitive dysfunction. As a step towards a better understanding of the mechanisms underlying behavioral changes and cognitive deficit associated with *T. gondii* infection, we used the global ultra-high-performance liquid chromatography-tandem mass spectrometry (UPLC/MS-MS) method to determine the changes in the metabolic profile of the hippocampus of mice infected by *T. gondii* infection at 7, 14, and 21 days post-infection (dpi).

## Materials and methods

### Parasite strain and animals

Cysts of *T. gondii* PRU (type II) strain were collected from the brain homogenates of Kunming mice that had been infected by the PRU strain for 1 month. Female, 3 weeks old, BALB/c mice were purchased from Lanzhou University Laboratory Animal Center (Lanzhou, China). This inbred mouse strain has been widely used as a preclinical model to understand the molecular and behavioral consequences of stress and neuropsychiatric disorders (Sathyanesan et al. 2017). Mice were housed in standard plastic cages in a humidity- and temperature-controlled room (22–25 °C), with a 12-h light–dark cycle. Mice had access to food and water ad libitum and were acclimatized for a week before being used in the investigation.

### Mouse infection

The mice ( $n = 36$ ) were randomly divided into six groups (6 mice/group): three infected groups and three control groups. Each mouse of the infected groups was inoculated orally with 10 *T. gondii* PRU cysts in 0.5 mL phosphate-buffered saline (PBS). Mice in the non-infected (control) groups received only 0.5 mL PBS without any *T. gondii* cysts (Torres et al. 2018; Zhang et al. 2020b). On days 7, 14, and 21 post-infection, one infected and the corresponding control group were euthanized by controlled CO<sub>2</sub> exposure followed by cervical dislocation. The brain was immediately harvested out of the mouse skull and the hippocampus region was dissected out using a dissecting microscope with a cold stage. The collected hippocampi were washed immediately with chilled PBS to remove the excess blood and any residual fluid was removed by bibulous paper, followed by storing the hippocampi at – 80 °C until analysis.

### Determination of *Toxoplasma gondii* infection in the brain

The presence of *T. gondii* in the hippocampus was examined using a PCR assay that targets the *T. gondii* *B1* gene. Briefly, the TIANamp Genomic DNA kit (TianGen™, Beijing, China) was used to isolate genomic DNA from ~ 10 mg of the hippocampus samples of infected and control mice. The extracted DNA was stored at – 20 °C until use. The PCR was performed with a T100™ Thermal Cycler (Bio-Rad, USA) using Premix Taq™ (Takara, Dalian, China). The PCR protocol including the primers was strictly performed as described previously (Ma et al. 2019).

## Metabolite extraction

The frozen hippocampi were transferred from  $-80\text{ }^{\circ}\text{C}$  to  $-20\text{ }^{\circ}\text{C}$  for 30 min and then defrosted at  $4\text{ }^{\circ}\text{C}$  (Gu et al. 2015; Lin et al. 2007; Zhang et al. 2020a). For metabolite extraction,  $\sim 25\text{ mg}$  of each defrosted hippocampus was mixed with  $800\text{ }\mu\text{l}$   $\text{H}_2\text{O}/\text{MeOH}$  (50:50% vol/vol) and lysed using TissueLyse bead-mill homogenizer (Qiagen, Hilden, Germany). The homogenized hippocampi were centrifuged to remove cellular debris at  $25,000g$  for 20 min at  $4\text{ }^{\circ}\text{C}$ . The supernatant of the homogenized hippocampi was collected and  $50\text{ }\mu\text{l}$  of the supernatant was used for metabolite extraction using SPE (solid-phase extraction) column (Strata-X polymeric reversed-phase column, Phenomenex, USA). The purified metabolites were dissolved with acetonitrile. To examine the reproducibility and reliability of the LC-MS/MS method,  $\sim 20\text{ }\mu\text{l}$  of each metabolite sample was pooled and examined as a QC sample.

## LC-MS/MS analysis

LC-MS/MS was performed using ultra-high-performance liquid chromatography (UPLC) system (Waters, Milford, USA). Reversed-phase separation was performed using ACQUITY UPLC BEH C18 column ( $100\text{ mm}\times 2.1\text{ mm}$ ,  $1.7\text{ }\mu\text{m}$ , Waters, UK) and the column oven was maintained at  $50\text{ }^{\circ}\text{C}$ . The flow rate was set as  $0.4\text{ ml/min}$  and the mobile phase consisted of two solvents: solvent A (water + 0.1% formic acid) and solvent B (acetonitrile + 0.1% formic acid). The metabolites were eluted by a chromatographic gradient elution process as follows: 100% solvent A for 0–2 min; 0–100% solvent B for  $\sim 11\text{ min}$ ; 100% solvent B for 11–13 min; and 100% solvent A for 13–15 min. A high-resolution tandem mass spectrometer SYNAPT G2 XS QTOF (Waters, Ireland) was used for the analysis of the eluted metabolites. For both positive ( $\text{ESI}^+$ ) and negative ( $\text{ESI}^-$ ) ion modes, the capillary and sampling cone voltages were set at 2 kV and 40 V, respectively. The mass to charge ratios ( $m/z$ ) between 50 and 1200 Da were recorded and the scan time was 0.2 s. Parent ion of the metabolite was fragmented using 20–40 eV and scan for 0.2 s.

## Metabolite identification, bioinformatics, and statistical analysis

Raw data processing, including peak alignment, normalization, and metabolite identification were carried out using Progenesis Q1 software. The  $m/z$  and retention time of the metabolite ions were mapped to the substance database of BGI-Shenzhen. Centroid MSE (mean square error) mode was used for data collection and analysis of the relative quantity of metabolites in both ( $\text{ESI}^+$ ) and ( $\text{ESI}^-$ ) ion modes. Differential metabolite (DM) analyses between infected and uninfected hippocampi were performed using Student's  $t$ -test and the metabolites with  $P$ -value  $< 0.05$  were deemed as DMs.

The identified DMs were mapped to HMDB (<http://www.hmdb.ca/>) and KEGG ([www.genome.jp/kegg/](http://www.genome.jp/kegg/)) to detect the pathways that are involved in the infection. SIMCA 13.0 software was used to perform multivariate statistical analysis and the normalized data of all metabolites were used as input data for partial least squares-discriminant analysis (PLS-DA). Weighted correlation network analysis (WGCNA) was performed to identify the metabolites that are significantly correlated with *T. gondii* infection in the hippocampi. In the WGCNA, infected samples were assigned 1, while non-infected control samples were assigned 0. Normalized abundance of the metabolites was used as input data for WGCNA, and the soft power that showed scale-free topology model fitting index  $R^2 > 0.8$  was selected for analysis of soft thresholding adjacency matrix of WGCNA. The WGCNA protocol was performed according to WGCNA tutorials (<https://horvath.genetics.ucla.edu/html/CoexpressionNetwork/Rpackages/WGCNA/Tutorials/index.html>). Receiver operating characteristic (ROC) test and area under the curve (AUC) were used to identify the potential biomarkers of the infected hippocampi. ROC and AUC were analyzed using pROC R package as described previously (Robin et al. 2011). The metabolites that were significantly associated with *T. gondii* infection with an AUC value  $> 0.7$  were deemed as potential biomarkers for *T. gondii* infection.

## Results

### Confirmation of *T. gondii* infection

At 14 dpi, all mice in the infected groups showed clear clinical manifestations, such as decreased appetite, hunched back and ruffled fur. However, at 21 dpi, all infected mice exhibited signs of recovery. All mice in control groups showed no clinical signs of infection at any time point in the experiment. All hippocampi of infected mice collected at 7 dpi, 14 dpi, and 21 dpi were *T. gondii B1* gene positive, whereas no amplified *B1* gene product was detected in the hippocampi of the non-infected mice (Fig. S1).

### Overall metabolic features of the infected hippocampi

A total of 3200 and 6198 metabolite ions were detected in the negative electrospray ionization ( $\text{ESI}^-$ ) mode and positive electrospray ionization ( $\text{ESI}^+$ ) mode, respectively. We examined whether the metabolic profiles of the infected hippocampi were different from that of the non-infected hippocampi using PLS-DA. In both  $\text{ESI}^-$  and  $\text{ESI}^+$  modes, the infected and non-infected hippocampi were clustered separately, indicating infection-specific metabolic signatures of the hippocampi (Fig. 1).

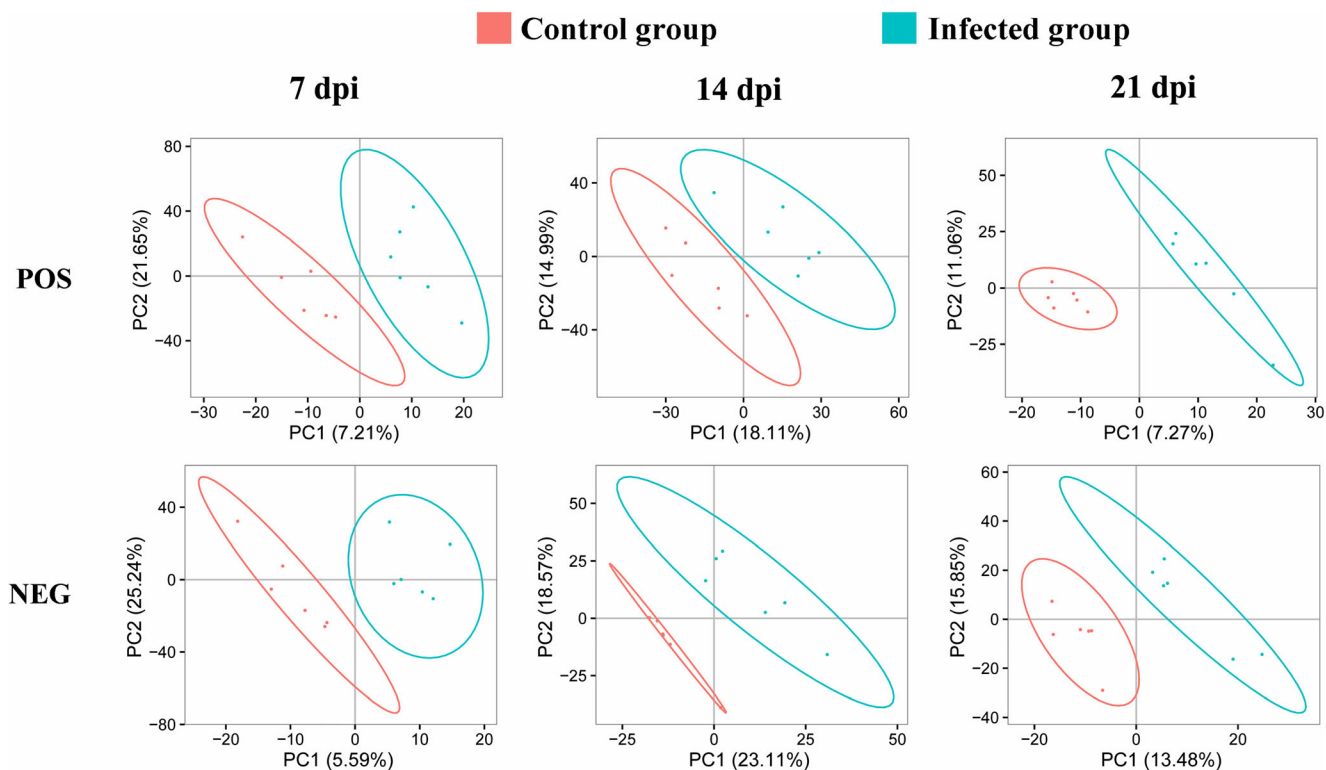


**Fig. 1** PLS-DA plots of the metabolomic features of the hippocampi of *T. gondii*-infected mice at 7, 14, and 21 dpi compared to those of the corresponding control mouse groups. POS and NEG denote the PLS-DA plots of the positive and negative ion modes, respectively. The number of dots within the plots corresponds to the number of analyzed hippocampal samples per mouse group

**Differential metabolites in the infected hippocampi**

We identified 25, 82, and 105 DMs in the infected hippocampi at 7 dpi, 14 dpi, and 21 dpi, respectively. Most of the DMs at 14 dpi and 21 dpi were upregulated (Fig. 2a). The details of the DMs are listed in Table S1. Intersection analysis showed that most of the DMs were time specific and only one common DM (sphingosyl-phosphocholine) was found at all three time points after infection (Fig. 2b). Five DMs were common

between 7 dpi and 21 dpi, including sphingosyl-phosphocholine, 2”,4”,6”-triacylglycitin, lecithin, tetrahydrocorticosterone, and trans-hexadec-2-enoyl carnitine. However, at 14 dpi and 21 dpi, 34 DMs were common. These included sphingosyl-phosphocholine, phosphatidylethanolamine, psychosine, arachidonic acid, palmitate, oleic acid, ricinoleic acid, tridecyl phloretate, stearyl glycine, linoelaidyl carnitine, L-palmitoylcarnitine, 2-arachidonylglycerol, cervonyl carnitine, ceramide (d18:1/

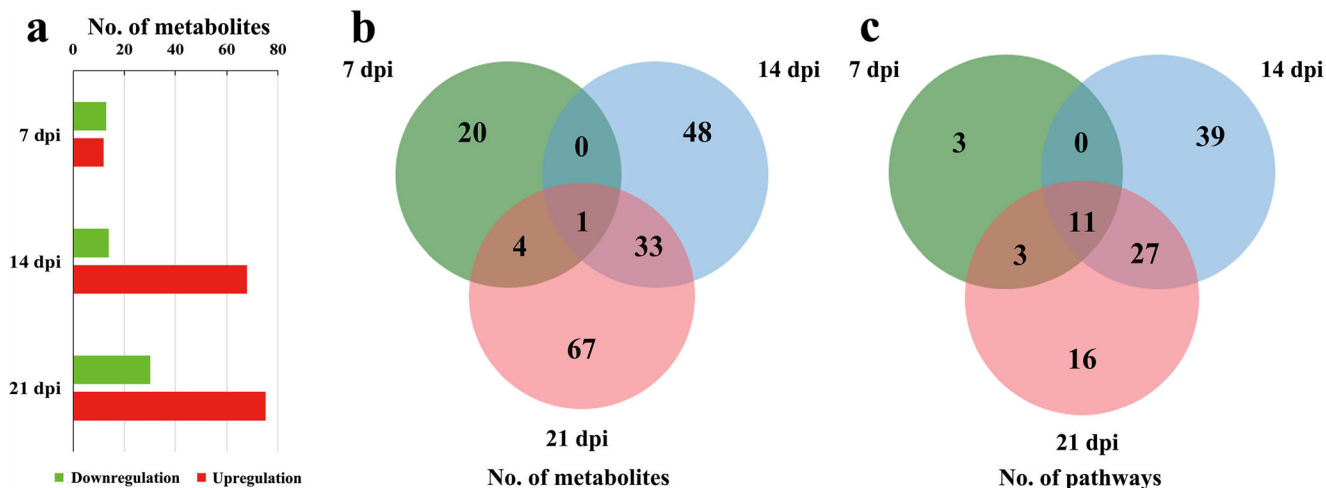


**Fig. 2** Differential metabolites (DMs) and the pathway numbers. **a** The number of DMs at 7, 14, and 21 dpi. **b** Venn diagram of the DMs showing the common and unique DMs at 7, 14, and 21 dpi. **c** Venn diagram of the number of pathways mapped to the DMs at 7, 14, and 21 dpi



16:0), 3alpha,7alpha,12alpha,26-tetrahydroxy-5beta-cholestane, calcitriol, heptadecanoyl carnitine, 3-hydroxytetradecanoyl carnitine, 3-hydroxy-9-hexadecenoylcarnitine, MG(22:2(13Z,16Z)/0:0/0:0), 2-hydroxymyristoylcarnitine, (17alpha,23S)-Epoxy-28,29-dihydroxy-27-norlanost-8-ene-3,24-dione, Istamycin A3, MG(20:3(5Z,8Z,11Z)/0:0/0:0), arachidyl carnitine, paederoside, leontogenin, Nb-palmitoyltryptamine, 12-hydroxy-12-octadecanoylcarnitine, 7alpha-hydroxy-3-oxo-4-cholestenolate, persin, methyl acetyl ricinoleate, SM(d18:0/16:1(9Z)), and 25-hydroxyvitamin D3-26,23-lactone.

### Hippocampus pathways affected by *T. gondii*

As shown in Fig. 2c, at 7 dpi, 14 dpi, and 21 dpi, the DMs were mapped to 17, 77, and 57 pathways, respectively. Three pathways were exclusively found at 7 dpi, including thiamine metabolism, sulfur relay system, and 2-oxocarboxylic acid metabolism. At 14 dpi, 39 pathways were exclusively identified, such as EGFR tyrosine kinase inhibitor resistance, MAPK signaling pathway, calcium signaling pathway, chemokine signaling pathway, NF-kappa B signaling pathway, VEGF signaling pathway, gap junction, natural killer cell-mediated cytotoxicity, T cell receptor signaling pathway, B

cell receptor signaling pathway, circadian entrainment, long-term potentiation, glutamatergic synapse, cholinergic synapse, dopaminergic synapse, estrogen signaling pathway, thyroid hormone signaling pathway, glioma, and non-small cell lung cancer. At 21 dpi, 16 pathways were exclusively detected, such as arginine and proline metabolism, D-arginine and D-ornithine metabolism, drug metabolism-cytochrome P450, histidine metabolism, biosynthesis of amino acids, pyruvate metabolism, galactose metabolism, starch and sucrose metabolism, pyrimidine metabolism, and purine metabolism. Although many altered pathways were related to a specific infection time, 11 pathways were common at 7, 14, and 21 dpi. These included neuroactive ligand-receptor interaction, retrograde endocannabinoid signaling, inflammatory mediator regulation of TRP channels, glycerophospholipid metabolism, arachidonic acid metabolism, linoleic acid metabolism, choline metabolism in cancer, sphingolipid metabolism, steroid hormone biosynthesis, glycosylphosphatidylinositol (GPI)-anchor biosynthesis, and regulation of autophagy. The relationships between DMs and the common 11 pathways are shown in Fig. 3, and the number of DMs in each of the 11 common pathways is shown in Table 1. Pathways were identified by at least 1 metabolite and most of the metabolites in these pathways were upregulated.

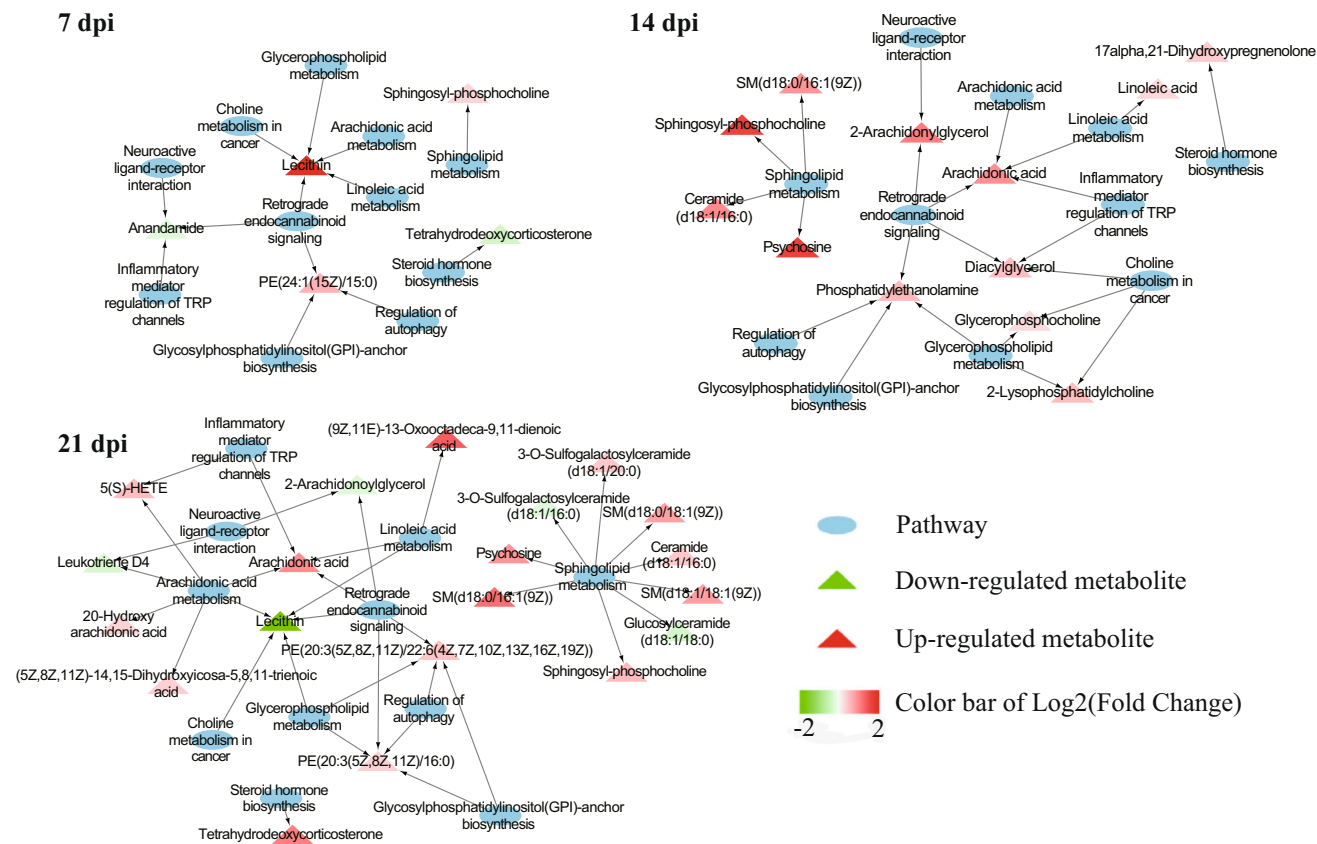


**Fig. 3** The relationships among differential metabolites and the 11 common pathways at 7, 14, and 21 dpi. Red and green triangles represent upregulated and downregulated metabolites, respectively. The blue ovals represent the pathways

**Table 1** The number of differentially abundant metabolites of the 11 common pathways

	7 dpi		14 dpi		21 dpi		Total Number
	Up	Down	Up	Down	Up	Down	
Sphingolipid metabolism	1	0	4	0	7	2	14
Retrograde endocannabinoid signaling	2	1	4	0	3	2	12
Arachidonic acid metabolism	1	0	1	0	4	2	8
Glycerophospholipid metabolism	2	0	3	0	2	1	8
Linoleic acid metabolism	1	0	2	0	2	1	6
Choline metabolism in cancer	1	0	3	0	0	1	5
Inflammatory mediator regulation of TRP channels	0	1	2	0	2	0	5
Glycosylphosphatidylinositol (GPI)-anchor biosynthesis	1	0	1	0	2	0	4
Regulation of autophagy	1	0	1	0	2	0	4
Neuroactive ligand-receptor interaction	0	1	1	0	0	2	4
Steroid hormone biosynthesis	0	1	1	0	1	0	3

## Identification of potential biomarkers for *T. gondii* infection

To further identify the metabolites that are strongly linked to *T. gondii* infection in the hippocampi, WGCNA was performed. A soft threshold power 4 was selected for WGCNA analysis to produce a hierarchical clustering dendrogram because it was the lowest power at which the scale-free topology fit index reached 0.8 (Fig. 4a). Additionally, soft threshold power 4 has a relatively high mean metabolite connectivity (Fig. 4b). Metabolites were categorized into 7 modules, including red, green, turquoise, brown, blue, yellow, and gray (Fig. 4c). As shown in Fig. 4d, the turquoise module was the most significantly associated with *T. gondii* infection (correlation index = 0.66, *P* value = 1e-05). In this module, 33 metabolites were significantly associated with *T. gondii* infection (Table 2). All 33 metabolites were upregulated in the infected hippocampi (Fig. 5). Of these, 30 metabolites showed an area under the ROC curve > 0.7 and were identified as potential infection-specific biomarkers (Fig. 6). These 30 potential biomarkers included leontogenin, arachidonic acid, sphingosyl-phosphocholine, linoelaidyl carnitine, 7 $\alpha$ -hydroxy-3-oxo-4-cholestenoate, 25-hydroxyvitamin D3-26,23-lactone, cervonyl carnitine, MG(20:3(5Z,8Z,11Z)/0:0/0:0), ricinoleic acid, 3-hydroxy-9-hexadecenoylcarnitine, 3-hydroxytetradecanoyl carnitine, MG(22:2(13Z,16Z)/0:0/0:0), persin, L-palmitoylcarnitine, arachidyl carnitine, 12-hydroxy-12-octadecanoylcarnitine, 3 $\alpha$ ,7 $\alpha$ ,12 $\alpha$ ,26-tetrahydroxy-5 $\beta$ -cholestane, 2-hydroxymyristoylcarnitine, Nb-palmitoyltryptamine, (17 $\alpha$ ,23S)-epoxy-28,29-dihydroxy-27-norlanost-8-ene-3,24-dione, calcitriol, heptadecanoyl carnitine, ceramide (d18:1/16:0), oleic acid, methyl acetyl ricinoleate, psychosine, (9S)-(10E,12Z,15Z)-9-hydroxyoctadecatri-10,12,15-enoic acid, Istimycin A3,

palmitate, and sandoricin. Pathway analysis showed that 12 of the potential biomarkers are involved in 32 pathways (Fig. 7).

## Discussion

We examined the differences in the hippocampal metabolic profiles between *T. gondii*-infected and uninfected BALB/c mice using an ultra-high-performance LC-MS/MS-based metabolomics approach. Clear differences were detected between the metabolic patterns of the hippocampus of infected and uninfected mice (Fig. 1). Infection induced significant metabolomic changes in the hippocampus, where 25, 82, and 105 DMs were detected in infected hippocampi at 7, 14, and 21 dpi, respectively. Previous studies have shown that the abundance of metabolites changed significantly (fold change 4–20) in mice post-mortem (Murphy 2010; Wasek et al. 2018). In the present study, only 9 out of the 137 identified differential metabolites had fold changes 4–8 (Table S1). Also, our results identified specific, altered metabolites and biochemical pathways that were specific to the hippocampi of infected mice compared with those of the control mice. Therefore, the limited metabolic alterations and their specific association with infection status suggest that the observed changes are not related to the post-mortem changes in metabolites. Additionally, the metabolic disturbances detected during *T. gondii* infection were consistent with the role played by the hippocampus in learning and memory processes, as discussed below.

Most of the identified DMs were time dependent; however, sphingosyl-phosphocholine was significantly upregulated in infected hippocampi at 7, 14, and 21 dpi, suggesting a crucial role of this metabolite in the neuropathogenesis of *T. gondii*

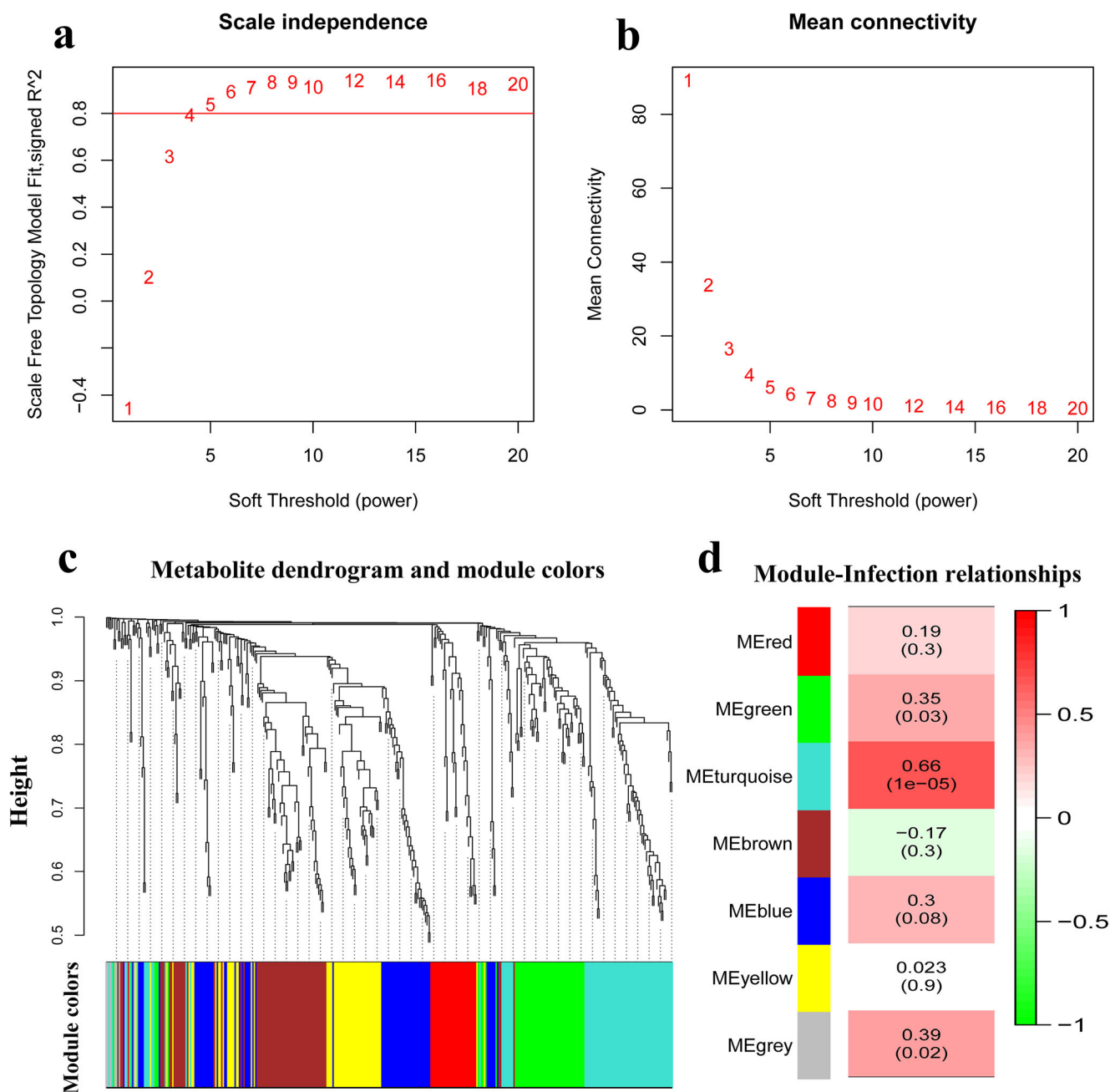


**Fig. 4** Weighted correlation network analysis, selection of the soft thresholding powers, and module detection of the metabolites. **a** The influence of different soft thresholding powers (x-axis) on scale-free topology fit index (y-axis). **b** The relationship between soft thresholding power (x-axis) and the mean connectivity (degree, y-axis), which shows

the strength of the connection between different metabolites. **c** Cluster dendrogram and assignment of functional modules (ME). Colors in the horizontal bar represent the modules. The branches correspond to modules of the highly interconnected groups of metabolites. **d** Global correlation index between the ME and *T. gondii* infection status.

infection. The behavioral changes related to schizophrenia are associated with alterations of glycerophospholipid metabolism in mice (Liang et al. 2019). Also, a reduction in glycerophospholipid metabolism is reported in schizophrenia, autism, and Down syndrome (Yu et al. 2020). Sphingosyl-phosphocholine, the deacylated derivative of sphingomyelin, is an important lipid mediator that plays a role in the regulation of brain functions (Nixon et al. 2008).

Previous studies have shown that the metabolism of sphingosyl-phosphocholine is associated with neurite outgrowth in mice (Sugiyama et al. 1993), via increasing AP-1 DNA-binding activity (Berger et al. 1995). Chronic stimulation by sphingosyl-phosphocholine also increases the proliferation of astrocytes and the release of neurotransmitter glutamate (Chiulli et al. 2007). Alteration of glutamate transportation and the resultant excitotoxicity of

**Table 2** The metabolites in mice hippocampi that were significantly associated with *Toxoplasma gondii* infection

Metabolites	Correlation index	P value of correlation index
Leontogenin	0.72	6.19E-07
Arachidonic acid	0.72	7.73E-07
Sphingosyl-phosphocholine	0.71	1.20E-06
MG(22:4(7Z,10Z,13Z,16Z)/0:0/0:0)	0.69	2.64E-06
7alpha-Hydroxy-3-oxo-4-cholestenoate	0.69	3.29E-06
25-Hydroxyvitamin D3-26,23-lactone	0.68	4.70E-06
Cervonyl carnitine	0.68	4.75E-06
MG(20:3(5Z,8Z,11Z)/0:0/0:0)	0.68	4.83E-06
Ricinoleic acid	0.68	6.20E-06
3-Hydroxy-9-hexadecenoylcarnitine	0.64	2.34E-05
3-Hydroxytetradecanoyl carnitine	0.64	2.97E-05
MG(22:2(13Z,16Z)/0:0/0:0)	0.62	5.27E-05
Persin	0.62	5.47E-05
L-Palmitoylcarnitine	0.61	8.33E-05
Arachidyl carnitine	0.60	0.000104
12-Hydroxy-12-octadecanoylcarnitine	0.60	0.000116
3alpha,7alpha,12alpha,26-Tetrahydroxy-5beta-cholestane	0.58	0.000215
2-Hydroxymyristoylcarnitine	0.57	0.000248
Nb-Palmitoyltryptamine	0.56	0.000353
(17alpha,23S)-Epoxy-28,29-dihydroxy-27-norlanost-8-ene-3,24-dione	0.54	0.000732
Calcitriol	0.52	0.001129
Heptadecanoyl carnitine	0.51	0.001455
Ceramide (d18:1/16:0)	0.51	0.001588
Oleic acid	0.48	0.002991
Methyl acetyl ricinoleate	0.47	0.003999
Psychosine	0.45	0.005539
(9S)-(10E,12Z,15Z)-9-Hydroxyoctadecatri-10,12,15-enoic acid	0.45	0.006051
Lstamycin A3	0.43	0.009683
(9Z,11E)-13-Oxo-octadeca-9,11-dienoic acid	0.42	0.011203
SM(d18:0/16:1(9Z))	0.42	0.011364
Paederoside	0.40	0.014782
Palmitate	0.40	0.015261
Sandoricin	0.33	0.049254

postsynaptic neurons have been shown in *T. gondii* infection (David et al. 2016; Mendez and Koshy 2017). Additionally, alteration of neuron subpopulations has been reported in *T. gondii*-infected pigs (Odorizzi et al. 2010).

To further identify the pathways that could contribute to the host behavioral alteration during *T. gondii* infection, all DMs of the infected hippocampi were mapped to the pathways in the KEGG database. As shown in Fig. 2c, 17, 77, and 57 pathways were enriched at 7, 14, and 21 dpi, respectively. A total of 11 common pathways were altered at all infection stages. Interestingly, most of the common pathways were related to neural activity, such as sphingolipid metabolism, retrograde endocannabinoid signaling, inflammatory mediator regulation of TRP channels, steroid hormone biosynthesis

pathway, arachidonic acid metabolism, and linoleic acid metabolism.

Pathway analysis showed that sphingosyl-phosphocholine is a crucial metabolite of sphingolipid metabolism pathway. Most of the DMs involved in the sphingolipid metabolism pathway were upregulated in the infected hippocampi and the number of DMs increased as infection progressed. At 7 dpi, sphingolipid pathway was regulated by one upregulated metabolite (sphingosyl-phosphocholine). At 14 dpi, the pathway was regulated by 4 DMs (upregulated psychosine, ceramide (d18:1/16:0), sphingosyl-phosphocholine and SM(d18:0/16:1(9Z))). At 21 dpi, this pathway was regulated by 9 DMs (including 7 upregulated psychosine, SM(d18:0/16:1(9Z)), SM(d18:1/18:1(9Z)), SM(d18:0/18:1(9Z)),



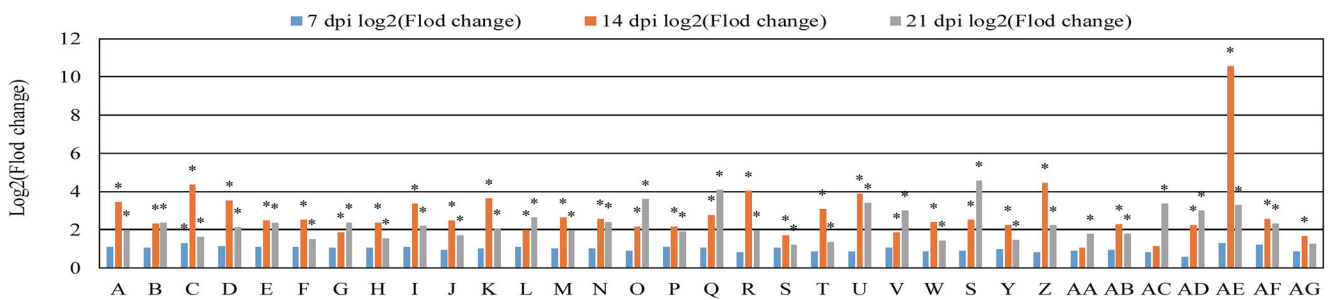


**Fig. 5** Log<sub>2</sub> (fold change) data of the metabolites that were significantly correlated with *T. gondii* infection. A: Leontogenin; B: arachidonic acid; C: sphingosyl-phosphocholine; D: linoelaidyl carnitine; E: 7 $\alpha$ -Hydroxy-3-oxo-4-cholestenoate; F: 25-hydroxyvitamin D3-26,23-lactone; G: cervonyl carnitine; H: MG(20:3(5Z,8Z,11Z)/0:0/0:0); I: ricinoleic acid; J: 3-hydroxy-9-hexadecenoylcarnitine; K: 3-hydroxytetradecanoyl carnitine; L: MG(22:2(13Z,16Z)/0:0/0:0); M: persin; N: L-palmitoylcarnitine; O: arachidyl carnitine; P: 12-hydroxy-12-octadecanoylcarnitine; Q: 3 $\alpha$ ,7 $\alpha$ ,12 $\alpha$ ,26-Tetrahydroxy-

5 $\beta$ -cholestane; R: 2-hydroxymyristoylcarnitine; S: N $\beta$ -palmitoyltryptamine; T: (17 $\alpha$ ,23S)-epoxy-28,29-dihydroxy-27-norlanost-8-ene-3,24-dione; U: calcitriol; V: heptadecanoyl carnitine; W: ceramide (d18:1/16:0); S: oleic acid; Y: methyl acetyl ricinoleate; Z: psychosine; AA: (9S)-(10E,12Z,15Z)-9-hydroxyoctadecatri-10,12,15-enoic acid; AB: Istamycin A3; AC: (9Z,11E)-13-oxooctadeca-9,11-dienoic acid; AD: SM(d18:0/16:1(9Z)); AE: paderoside; AF: palmitate; and AG: sandoricin; \**p* value < 0.05

sphingosyl-phosphocholine, ceramide (d18:1/16:0), 3-O-sulfogalactosylceramide (d18:1/20:0), and 2 downregulated glucosylceramide (d18:1/18:0), 3-O-sulfogalactosylceramide (d18:1/16:0)) (Table 1 and Fig. 3).

Several DMs of the sphingolipid metabolism pathway regulate neuronal function. For example, the neurotoxic lysosphingolipid psychosine is a by-product of galactosylceramide metabolism and can disrupt lipid rafts and vesicular transport, all are critical processes for the function of glia and neurons (Spassieva and Bieberich 2016). Accumulation of psychosine induces apoptosis in murine oligodendrocyte progenitor cells (Zaka and Wenger 2004). Also, ceramide and glucosylceramide play a role in the regulation of the progression of different neurodegenerative diseases (Farfel-Becker et al. 2014; Mencarelli and Martinez-Martinez 2013). Given that sphingosyl-phosphocholine and sphingolipid metabolism were altered during acute and chronic infections, and given their abovementioned neuroregulatory functions, it is possible that they are implicated in the pathophysiology of behavior alteration in the infected mice.

*Toxoplasma gondii* infection is infamous for causing loss of aversion of rodents to the cat urine, which might be related to disruption of the innate anti-predator adrenocorticotrophic hormonal response (Yin et al. 2017), increase in testosterone synthesis mediated by steroid hormones (Vyas 2015), or dysregulation of anxiety, stress, and fear, which are mediated by the endocannabinoid system (Lutz et al. 2015). The endocannabinoid signaling pathway was shown to reduce the GABAergic synaptic transmission to gonadotropin-releasing hormone neurons (Farkas et al. 2010). In our study, the metabolites linked to the steroid hormone biosynthesis pathway and retrograde endocannabinoid signaling pathway were altered in the infected hippocampi (Fig. 3). In the steroid hormone biosynthesis pathway, tetrahydrodeoxycorticosterone was downregulated at 7 dpi but was upregulated at 21 dpi, and 17 $\alpha$ ,21-dihydroxypregnenolone was upregulated at 14 dpi. In the

retrograde endocannabinoid signaling pathway, two significantly altered metabolites (downregulated anandamide and upregulated lecithin) were detected at 7 dpi. At 14 dpi, four upregulated metabolites (phosphatidylethanolamine, diacylglycerol, 2-arachidonoylglycerol, and arachidonic acid) were detected.

At 21 dpi, there were three upregulated metabolites ((PE(20:3(5Z,8Z,11Z)/22:6(4Z,7Z,10Z,13Z,16Z,19Z))), PE(20:3(5Z,8Z,11Z)/16:0), and arachidonic acid) and two downregulated metabolites (lecithin and 2-arachidonoylglycerol). The 2-arachidonoylglycerol and anandamide play roles in the regulation of synaptic functions and plasticity, learning and memory, reward and addiction, antinociception, and anxiety (Luchicchi and Pistis 2012). They can also inhibit the release of neurotransmitters, such as  $\gamma$ -aminobutyric acid (GABA) and glutamate in the hippocampi (Gerdeman and Lovinger 2001; Hoffman and Lupica 2000; Piomelli 2003). Furthermore, phosphatidylethanolamine regulates the biosynthesis of endocannabinoids (Leung et al. 2006) and arachidonic acid plays a role in the regulation of neurological and immune responses (Bosetti 2007; Grimbale and Tappia 1998; Levick et al. 2007). The alterations of the aforementioned metabolites in the steroid hormone biosynthesis and retrograde endocannabinoid signaling pathways are consistent with the adverse effects of infection on mouse learning and memory, which may contribute to the loss of innate aversion to cat urine (Evans et al. 2014; Ingram et al. 2013).

Transient receptor potential (TRP) channels are ligand-gated ion channels that act as transducers for thermal, chemical, and mechanical stimuli, and play roles in the regulation of immunomodulatory neuropeptide release, chronic pain, thermoregulation, and nociception (Shibasaki et al. 2007). TRP channels are directly modulated by immune cytokines and other inflammatory mediators. In the present study, the endogenous cannabinoid anandamide that serves as an agonist of human ligand-gated ion channel vanilloid receptor, which plays a role in nociception

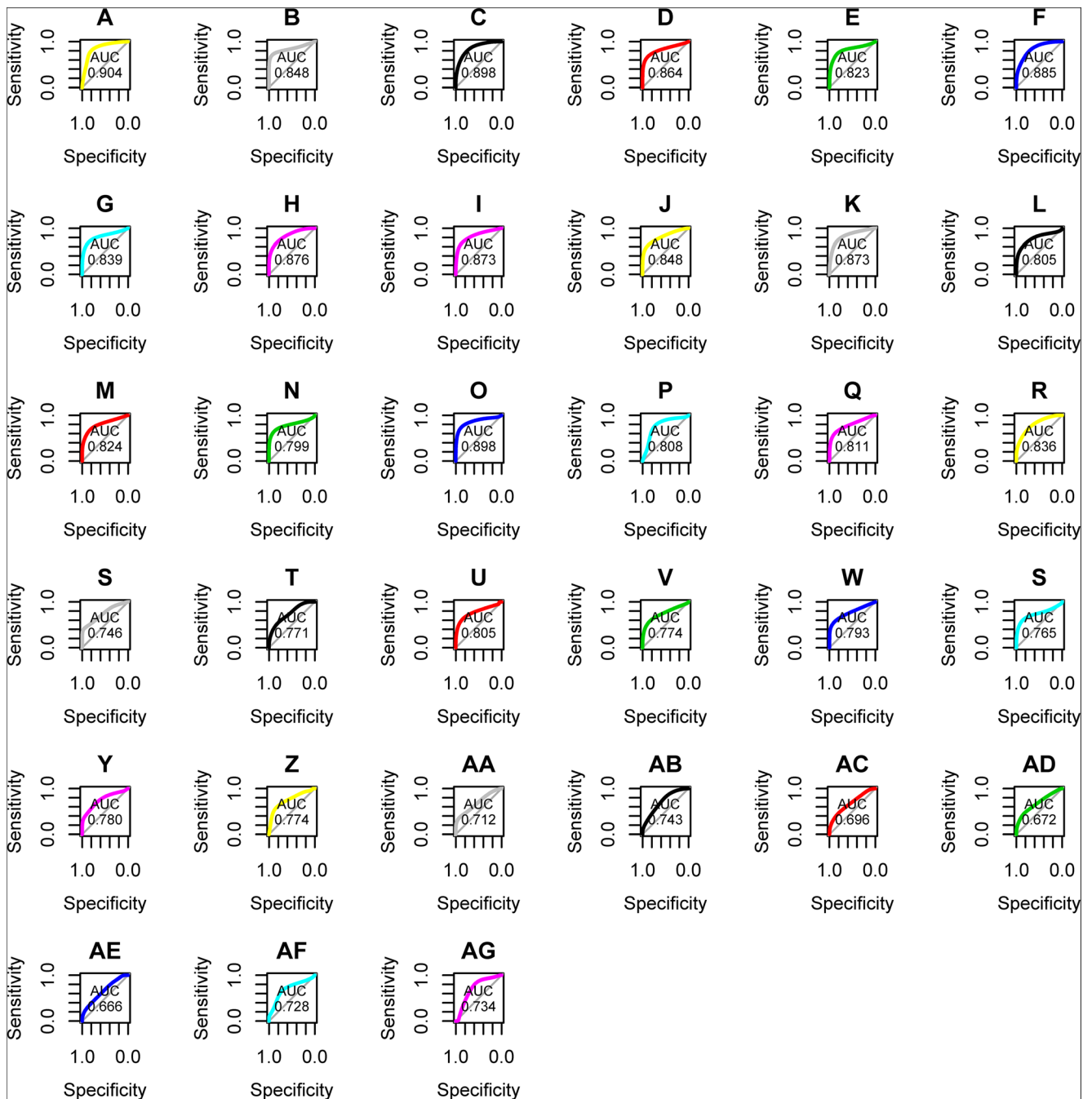


**Fig. 6** Receiver operating characteristics curve analysis of 33 metabolites that were significantly correlated with *T. gondii* infection. A: leontogenin; B: arachidonic acid; C: sphingosyl-phosphocholine; D: linoelaidyl carnitine; E: 7 $\alpha$ -hydroxy-3-oxo-4-cholestenolate; F: 25-hydroxyvitamin D3-26,23-lactone; G: cervonyl carnitine; H: MG(20:3(5Z,8Z,11Z)/0:0/0:0); I: ricinoleic acid; J: 3-hydroxy-9-hexadecenoylcarnitine; K: 3-hydroxytetradecanoyl carnitine; L: MG(22:2(13Z,16Z)/0:0/0:0); M: persin; N: L-palmitoylcarnitine; O: arachidyl carnitine; P: 12-hydroxy-12-octadecanoylcarnitine; Q: 3 $\alpha$ ,7 $\alpha$ ,12 $\alpha$ ,26-Tetrahydroxy-

5 $\beta$ -cholestane; R: 2-hydroxymyristoylcarnitine; S: Nb-palmitoyltryptamine; T: (17 $\alpha$ ,23S)-Epoxy-28,29-dihydroxy-27-norlanost-8-ene-3,24-dione; U: calcitriol; V: heptadecanoyl carnitine; W: ceramide (d18:1/16:0); X: oleic acid; Y: methyl acetyl ricinoleate; Z: psychosine; AA: (9S)-(10E,12Z,15Z)-9-hydroxyoctadecatri-10,12,15-enoic acid; AB: Istamycin A3; AC: (9Z,11E)-13-oxooctadeca-9,11-dienoic acid; AD: SM(d18:0/16:1(9Z)); AE: paderoside; AF: palmitate; and AG: sandoricin

and regulation of feeding behavior, and neural generation of motivation and pleasure, was downregulated at 7 dpi. The downregulation of this metabolite at 7 dpi seems to underpin the pain associated with acute infection. At 14 dpi, arachidonic acid and

diacylglycerol were upregulated, and arachidonic acid and 5(S)-HETE were upregulated at 21 dpi (Fig. 3). Arachidonic acid, 5(S)-HETE, and diacylglycerol are important inflammatory mediators (Balboa et al. 2019; Bittleman and Casale 1995).

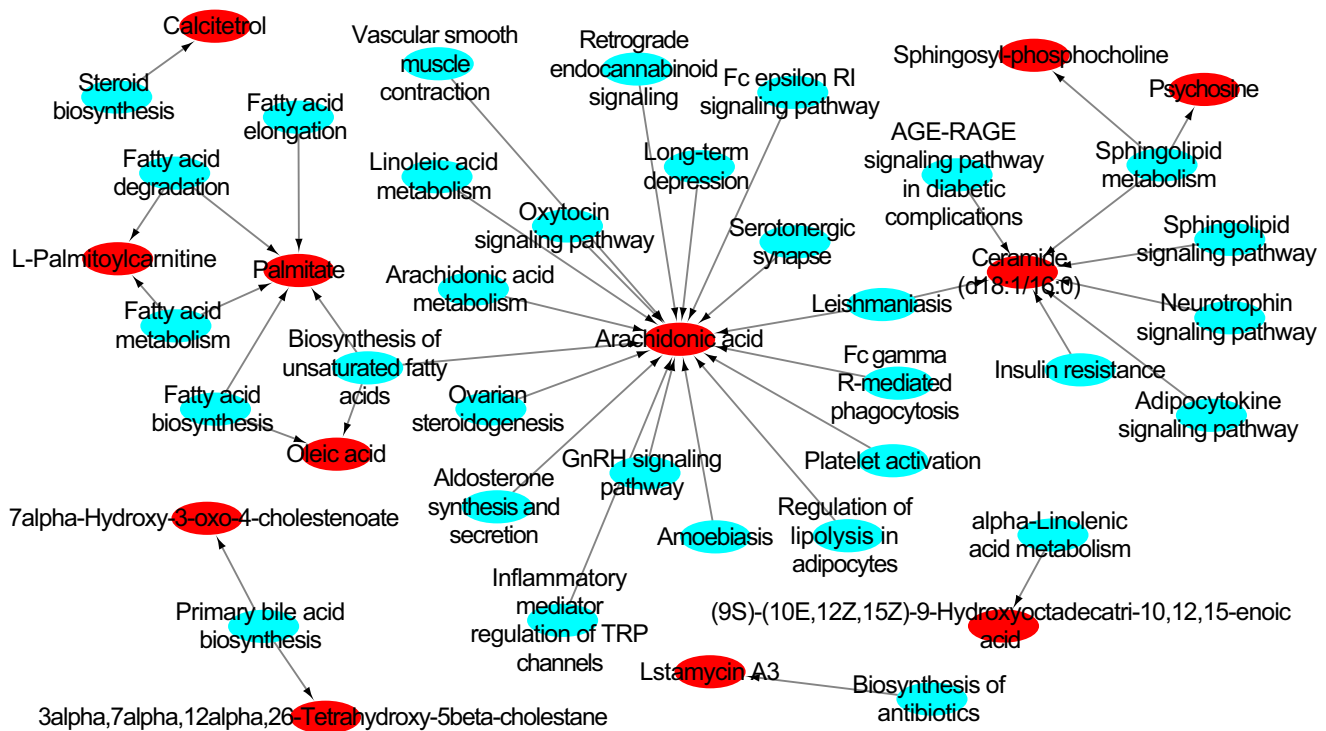


**Fig. 7** The relationship between potential biomarker metabolites and the associated regulatory pathways. Blue and red ovals represent the pathways and the potential biomarkers, respectively

Diacylglycerol is also involved in dopaminergic and glutamatergic synapse pathways (Table S1). Therefore, the increase of these inflammatory mediators at 14 and 21 dpi seem to play a dual role in limiting the parasite proliferation while promoting latent toxoplasmosis, which contributes to neurocognitive manifestations particularly memory impairment in the infected rats (Daniels et al. 2015).

In humans, brain infection with *T. gondii* is associated with Th1 immune response and production of proinflammatory factors (e.g., interleukin (IL)-1, IL-6, tumor necrosis factor- $\alpha$ , and inducible nitric oxide synthase) which are related to anxiety and depression disorder (Gale et al. 2014). A correlation was found between stress-related inflammation and alterations in the functions of the excitatory neurotransmitter glutamate in the hippocampus and behavioral abnormalities in BALB/c (Sathyanesan et al. 2017). Also, *T. gondii* caused anxiety-like symptoms and impaired cognitive functions in BALB/c mice. These adverse effects were ameliorated with pioglitazone, which attenuates oxidative damage and inflammation (Mahmoudvand et al. 2015). Therefore, metabolites of the inflammatory mediator regulation of the TRP channels pathway identified in the present study may play a role in the neurogenic inflammation that underpins the pathophysiology of both toxoplasmosis and behavioral modification. Further investigation of the effect of the interplay between *T. gondii* infection, inflammatory mediator regulation of TRP channels, and body temperature in hippocampus on the host behavior is warranted.

Our WGCNA analysis identified a subset of 33 hippocampus metabolites that may serve as potential biomarkers for cerebral toxoplasmosis (correlation index = 0.66,  $P$  value =  $1e-05$ ). The 33 metabolites responsive to *T. gondii* infection were all upregulated in the infected hippocampi (Fig. 5). We tested the sensitivity and specificity of the 33 metabolites using ROC analysis. As shown in Fig. 6, 30 of the 33 metabolites had an area under curve > 0.7, suggesting that these 30 metabolites are good candidates for predicting *T. gondii* infection. Leontogenin had the highest correlation value (correlation index = 0.72,  $P$  value =  $6.19E-07$ ) and AUC value (AUC = 0.90). However, the role of this metabolite in the neuropathogenesis of *T. gondii* or behavioral abnormalities is unknown. Arachidonic acid has been identified as a potential biomarker in previous metabolomic studies of *T. gondii* infection (Chen et al. 2018; Chen et al. 2017; Ma et al. 2020; Ma et al. 2019; Zhou et al. 2015; Zhou et al. 2016). In agreement with the previous studies, arachidonic acid was also significantly associated with *T. gondii* infection in the hippocampi (correlation index = 0.72,  $P$  =  $7.73E-07$ ). Arachidonic acid was involved in 4 (arachidonic acid metabolism, inflammatory mediator regulation of TRP channels, linoleic acid metabolism, and retrograde endocannabinoid signaling) out of the 11 common pathways.

All the identified potential biomarkers were mapped to the KEGG pathway database in order to identify their function. Twelve of the potential biomarkers were involved in 32 KEGG pathways (Fig. 7). Arachidonic acid was found to

regulate most of these pathways; however, sphingolipid metabolism pathway was regulated by three potential biomarkers (ceramide (d18:1/16:0), psychosine, and sphingosyl-phosphocholine). Arachidonic acid regulates various neurological and immunological mechanisms (Bosetti 2007; Grimble and Tappia 1998; Levick et al. 2007). Ceramide (d18:1/16:0) is involved in inflammatory processes and neurodegenerative diseases (Gertow et al. 2014; Mencarelli and Martinez-Martinez 2013). Alterations of psychosine and sphingosyl-phosphocholine can disrupt the sphingolipid metabolism, resulting in neurotoxicity (Sugiyama et al. 1993; Zaka and Wenger 2004). Further characterization of these potential biomarkers should expand our understanding of their roles in both *T. gondii* infection and behavioral modifications in the infected hosts.

## Conclusions

This is the first study to characterize the global metabolic changes in mouse hippocampus following *T. gondii* infection. The metabolomic profiles of the infected hippocampi were significantly different from that of the non-infected hippocampi. Although most of the differentially abundant metabolites were related to a certain stage of infection, sphingosyl-phosphocholine and 11 metabolic pathways were commonly detected at all stages of infection. Most of these common pathways are related to neuronal functions and/or immune responses, which play roles in the neuropathogenesis of *T. gondii* infection and in the neurobiology of behavioral abnormalities. We also identified a panel of 33 metabolites strongly correlated with infection and 30 of these were identified as potential biomarkers for *T. gondii* infection. Future research is required to validate the clinical predictive utility of the identified biomarkers.

**Supplementary Information** The online version contains supplementary material available at <https://doi.org/10.1007/s00436-021-07222-8>.

**Acknowledgements** The authors would like to acknowledge the technical assistance, including metabolite extraction, identification, and quantification, provided by BGI-Shenzhen, China.

**Funding** This work was supported, in part, by the National Natural Science Foundation of China (Grant No. 31902291), the National Key Research and Development Program of China (Grant No. 2017YFD0500403), the Yunnan Expert Workstation (Grant No. 202005AF150041), and the Veterinary Public Health Innovation Team of Yunnan Province.

**Data availability** The metabolomics raw data have been deposited in the MetaboLights database (Access number: MTBLS1890).

**Declarations** All mice were handled strictly in accordance with the Animal Ethics Procedures and Guidelines of the People's Republic of

China. The study's protocol was reviewed and approved by the Animal Ethics Committee of Lanzhou Veterinary Research Institute, Chinese Academy of Agricultural Sciences (Permit No. LVRIAEC2017-06).

**Competing interests** The authors declare no competing interests.

## References

- Abdoli A, Dalimi A (2014) Are there any relationships between latent *Toxoplasma gondii* infection, testosterone elevation, and risk of autism spectrum disorder? *Front Behav Neurosci* 8:339
- Balboa MA, de Pablo N, Meana C, Balsinde J (2019) The role of lipins in innate immunity and inflammation. *Biochim Biophys Acta Mol Cell Biol Lipids* 1864(10):1328–1337
- Bedny M, Caramazza A, Grossman E, Pascual-Leone A, Saxe R (2008) Concepts are more than percepts: the case of action verbs. *J Neurosci* 28(44):11347–11353
- Berenreiterova M, Flegr J, Kubena AA, Nemeč P (2011) The distribution of *Toxoplasma gondii* cysts in the brain of a mouse with latent toxoplasmosis: implications for the behavioral manipulation hypothesis. *PLoS One* 6(12):e28925
- Berger A, Rosenthal D, Spiegel S (1995) Sphingosylphosphocholine, a signaling molecule which accumulates in Niemann-Pick disease type A, stimulates DNA-binding activity of the transcription activator protein AP-1. *Proc Natl Acad Sci U S A* 92(13):5885–5889
- Binder JR, Westbury CF, McKiernan KA, Possing ET, Medler DA (2005) Distinct brain systems for processing concrete and abstract concepts. *J Cogn Neurosci* 17(6):905–917
- Bittleman DB, Casale TB (1995) 5-Hydroxyeicosatetraenoic acid (HETE)-induced neutrophil transcellular migration is dependent upon enantiomeric structure. *Am J Respir Cell Mol Biol* 12(3):260–267
- Boillat M et al (2020) Neuroinflammation-associated aspecific manipulation of mouse predator fear by *Toxoplasma gondii*. *Cell Reports* 30(2):320–334.e326
- Bosetti F (2007) Arachidonic acid metabolism in brain physiology and pathology: lessons from genetically altered mouse models. *J Neurochem* 102(3):577–586
- Chen XQ, Elsheikha HM, Hu RS, Hu GX, Guo SL, Zhou CX, Zhu XQ (2018) Hepatic metabolomics investigation in acute and chronic murine toxoplasmosis. *Front Cell Infect Microbiol* 8:189
- Chen XQ, Zhou CX, Elsheikha HM, He S, Hu GX, Zhu XQ (2017) Profiling of the perturbed metabolomic state of mouse spleen during acute and chronic toxoplasmosis. *Parasit Vectors* 10(1):339
- Chiulli N, Codazzi F, Di Cesare A, Gravaghi C, Zaccchetti D, Grohovaz F (2007) Sphingosylphosphocholine effects on cultured astrocytes reveal mechanisms potentially involved in neurotoxicity in Niemann-Pick type A disease. *Eur J Neurosci* 26(4):875–881
- da Silva RC, Langoni H (2009) *Toxoplasma gondii*: host-parasite interaction and behavior manipulation. *Parasitol Res* 105(4):893–898
- Daniels BP, Sestito SR, Rouse ST (2015) An expanded task battery in the Morris water maze reveals effects of *Toxoplasma gondii* infection on learning and memory in rats. *Parasitol Int* 64(1):5–12
- David CN, Frias ES, Szu JI, Vieira PA, Hubbard JA, Lovelace J, Michael M, Worth D, McGovern KE, Ethell IM, Stanley BG, Korzus E, Fiacco TA, Binder DK, Wilson EH (2016) GLT-1-dependent disruption of CNS glutamate homeostasis and neuronal function by the protozoan parasite *Toxoplasma gondii*. *PLoS Pathog* 12(6):e1005643
- Elsheikha HM, Busselberg D, Zhu XQ (2016) The known and missing links between *Toxoplasma gondii* and schizophrenia. *Metab Brain Dis* 31(4):749–759



- Evans AK, Strassmann PS, Lee IP, Sapolsky RM (2014) Patterns of *Toxoplasma gondii* cyst distribution in the forebrain associate with individual variation in predator odor avoidance and anxiety-related behavior in male Long-Evans rats. *Brain Behav Immun* 37:122–133
- Farfel-Becker T, Vitner EB, Kelly SL, Bame JR, Duan J, Shinder V, Merrill AH, Dobrenis K, Futerman AH (2014) Neuronal accumulation of glucosylceramide in a mouse model of neuronopathic Gaucher disease leads to neurodegeneration. *Hum Mol Genet* 23(4):843–854
- Farkas I, Kalló I, Deli L, Vida B, Hrabovszky E, Fekete C, Moenter SM, Watanabe M, Liposits Z (2010) Retrograde endocannabinoid signaling reduces GABAergic synaptic transmission to gonadotropin-releasing hormone neurons. *Endocrinology* 151(12):5818–5829
- Gale SD, Brown BL, Berrett A, Erickson LD, Hedges DW (2014) Association between latent toxoplasmosis and major depression, generalised anxiety disorder and panic disorder in human adults. *Folia Parasitol (Praha)* 61(4):285–292
- Gerdeman G, Lovinger DM (2001) CB1 cannabinoid receptor inhibits synaptic release of glutamate in rat dorsolateral striatum. *J Neurophysiol* 85(1):468–471
- Gertow J, Kjellqvist S, Ståhlman M, Cheung L, Gottfries J, Werngren O, Borén J, Franco-Cereceda A, Eriksson P, Fisher RM (2014) Ceramides are associated with inflammatory processes in human mediastinal adipose tissue. *Nutr Metab Cardiovasc Dis* 24(2):124–131
- Grimble RF, Tappia PS (1998) Modulation of pro-inflammatory cytokine biology by unsaturated fatty acids. *Z Ernährungswiss* 37(Suppl 1):57–65
- Groer MW et al (2011) Prenatal depression and anxiety in *Toxoplasma gondii*-positive women. *Am J Obstet Gynecol* 204(5):433 e431–433 e437
- Gu H, Zhang P, Zhu J, Raftery D (2015) Globally optimized targeted mass spectrometry: Reliable metabolomics analysis with broad coverage. *Anal Chem* 87(24):12355–12362
- He JJ, Ma J, Wang JL, Zhang FK, Li JX, Zhai BT, Wang ZX, Elsheikha HM, Zhu XQ (2019) Global transcriptome profiling of multiple porcine organs reveals *Toxoplasma gondii*-induced transcriptional landscapes. *Front Immunol* 10:1531
- Hoffman AF, Lupica CR (2000) Mechanisms of cannabinoid inhibition of GABA(A) synaptic transmission in the hippocampus. *J Neurosci* 20(7):2470–2479
- Hsu PC, Groer M, Beckie T (2014) New findings: depression, suicide, and *Toxoplasma gondii* infection. *J Am Assoc Nurse Pract* 26(11):629–637
- Huth AG, de Heer WA, Griffiths TL, Theunissen FE, Gallant JL (2016) Natural speech reveals the semantic maps that tile human cerebral cortex. *Nature* 532(7600):453–458
- Ingram WM, Goodrich LM, Robey EA, Eisen MB (2013) Mice infected with low-virulence strains of *Toxoplasma gondii* lose their innate aversion to cat urine, even after extensive parasite clearance. *PLoS One* 8(9):e75246
- Leung D, Saghatelian A, Simon GM, Cravatt BF (2006) Inactivation of N-acyl phosphatidylethanolamine phospholipase D reveals multiple mechanisms for the biosynthesis of endocannabinoids. *Biochemistry* 45(15):4720–4726
- Levick SP, Loch DC, Taylor SM, Janicki JS (2007) Arachidonic acid metabolism as a potential mediator of cardiac fibrosis associated with inflammation. *J Immunol* 178(2):641–646
- Li C, Wang A, Wang C, Ramamurthy J, Zhang E, Guadagno E, Trakadis Y (2018) Metabolomics in patients with psychosis: a systematic review. *Am J Med Genet B Neuropsychiatr Genet* 177(6):580–588
- Liang W, Huang Y, Tan X, Wu J, Duan J, Zhang H, Yin B, Li Y, Zheng P, Wei H, Xie P (2019) Alterations of glycerophospholipid and fatty acyl metabolism in multiple brain regions of schizophrenia microbiota recipient mice. *Neuropsychiatr Dis Treat* 15:3219–3229
- Lin CY, Wu H, Tjeerdema RS, Viant MR (2007) Evaluation of metabolite extraction strategies from tissue samples using NMR metabolomics. *Metabolomics* 3(1):55–67
- Luchicchi A, Pistis M (2012) Anandamide and 2-arachidonoylglycerol: pharmacological properties, functional features, and emerging specificities of the two major endocannabinoids. *Mol Neurobiol* 46(2):374–392
- Lutz B, Marsicano G, Maldonado R, Hillard CJ (2015) The endocannabinoid system in guarding against fear, anxiety and stress. *Nat Rev Neurosci* 16(12):705–718
- Ma J, He JJ, Hou JL, Zhou CX, Elsheikha HM, Zhu XQ (2020) Ultra performance liquid chromatography-tandem mass spectrometry-based metabolomics reveals metabolic alterations in the mouse cerebellum during *Toxoplasma gondii* infection. *Front Microbiol* 11:1555
- Ma J, He JJ, Hou JL, Zhou CX, Zhang FK, Elsheikha HM, Zhu XQ (2019) Metabolomic signature of mouse cerebral cortex following *Toxoplasma gondii* infection. *Parasit Vectors* 12(1):373
- Mahmoudvand H, Ziaali N, Aghaei I, Sheibani V, Shojaei S, Keshavarz H, Shabani M (2015) The possible association between *Toxoplasma gondii* infection and risk of anxiety and cognitive disorders in BALB/c mice. *Pathog Glob Health* 109(8):369–376
- Marra CM (2018) Central nervous system infection with *Toxoplasma gondii*. *Handb Clin Neurol* 152:117–122
- Mencarelli C, Martinez-Martinez P (2013) Ceramide function in the brain: when a slight tilt is enough. *Cell Mol Life Sci* 70(2):181–203
- Mendez OA, Koshy AA (2017) *Toxoplasma gondii*: Entry, association, and physiological influence on the central nervous system. *PLoS Pathog* 13(7):e1006351
- Mendoza J, Pevet P, Felder-Schmittbuhl MP, Bailly Y, Challet E (2010) The cerebellum harbors a circadian oscillator involved in food anticipation. *J Neurosci* 30(5):1894–1904
- Murphy EJ (2010) Brain fixation for analysis of brain lipid-mediators of signal transduction and brain eicosanoids requires head-focused microwave irradiation: an historical perspective. *Prostaglandins Other Lipid Mediat* 91(3–4):63–67
- Nixon GF, Mathieson FA, Hunter I (2008) The multi-functional role of sphingosylphosphorylcholine. *Prog Lipid Res* 47(1):62–75
- Odorizzi L, Moreira NM, Goncalves GF, da Silva AV, Sant'ana Dde M, Araujo EJ (2010) Quantitative and morphometric changes of subpopulations of myenteric neurons in swines with toxoplasmosis. *Auton Neurosci* 155(1–2):68–72
- Piomelli D (2003) The molecular logic of endocannabinoid signalling. *Nat Rev Neurosci* 4(11):873–884
- Reeber SL, Otis TS, Sillitoe RV (2013) New roles for the cerebellum in health and disease. *Front Syst Neurosci* 7:83
- Robin X, Turck N, Hainard A, Tiberti N, Lisacek F, Sanchez JC, Müller M (2011) pROC: an open-source package for R and S+ to analyze and compare ROC curves. *BMC Bioinformatics* 12:77
- Sathyanesan M, Haiar JM, Watt MJ, Newton SS (2017) Restraint stress differentially regulates inflammation and glutamate receptor gene expression in the hippocampus of C57BL/6 and BALB/c mice. *Stress* 20(2):197–204
- Shibasaki K, Suzuki M, Mizuno A, Tominaga M (2007) Effects of body temperature on neural activity in the hippocampus: regulation of resting membrane potentials by transient receptor potential vanilloid 4. *J Neurosci* 27(7):1566–1575
- Spasieva S, Bieberich E (2016) Lysosphingolipids and sphingolipidoses: psychosine in Krabbe's disease. *J Neurosci Res* 94(11):974–981
- Sugiyama E, Uemura K, Hara A, Taketomi T (1993) Metabolism and neurite promoting effect of exogenous sphingosylphosphocholine in cultured murine neuroblastoma cells. *J Biochem* 113(4):467–472
- Tenter AM, Heckerth AR, Weiss LM (2000) *Toxoplasma gondii*: from animals to humans. *Int J Parasitol* 30(12–13):1217–1258
- Torres L, Robinson SA, Kim DG, Yan A, Cleland TA, Bynoe MS (2018) *Toxoplasma gondii* alters NMDAR signaling and induces signs of



- Alzheimer's disease in wild-type, C57BL/6 mice. *J Neuroinflammation* 15(1):57
- Vyas A (2015) Mechanisms of host behavioral change in *Toxoplasma gondii* rodent association. *PLoS Pathog* 11(7):e1004935
- Wasek B, Aming E, Bottiglieri T (2018) The use of microwave irradiation for quantitative analysis of neurotransmitters in the mouse brain. *J Neurosci Methods* 307:188–193
- Wilkins JM, Trushina E (2017) Application of metabolomics in alzheimer's disease. *Front Neurol* 8:719
- Yin B, Gu C, Lu Y, Hegab IM, Yang S, Wang A, Wei W (2017) Repeated exposure to cat urine induces complex behavioral, hormonal, and c-fos mRNA responses in Norway rats (*Rattus norvegicus*). *Naturwissenschaften* 104(7-8):64
- Yu Q, He Z, Zubkov D, Huang S, Kurochkin I, Yang X, Halene T, Willmitzer L, Giavalisco P, Akbarian S, Khaitovich P (2020) Lipidome alterations in human prefrontal cortex during development, aging, and cognitive disorders. *Mol Psychiatry* 25(11):2952–2969
- Zaka M, Wenger DA (2004) Psychosine-induced apoptosis in a mouse oligodendrocyte progenitor cell line is mediated by caspase activation. *Neurosci Lett* 358(3):205–209
- Zhang H, He W, Huang Y, Zeng Z, Yang X, Huang H, Wen J, Cao Y, Sun H (2019) Hippocampal metabolic alteration in rat exhibited susceptibility to prenatal stress. *J Affect Disord* 259:458–467
- Zhang X, Dong J, Raftery D (2020a) Five easy metrics of data quality for LC-MS-based global metabolomics. *Anal Chem* 92(19):12925–12933
- Zhang Z et al (2020b) Identification of *Toxoplasma gondii* tyrosine hydroxylase (TH) activity and molecular immunoprotection against toxoplasmosis. *Vaccines (Basel)* 8(2)
- Zhou CX, Zhou DH, Elsheikha HM, Liu GX, Suo X, Zhu XQ (2015) Global metabolomic profiling of mice brains following experimental infection with the cyst-forming *Toxoplasma gondii*. *PLoS One* 10(10):e0139635
- Zhou CX, Zhou DH, Elsheikha HM, Zhao Y, Suo X, Zhu XQ (2016) Metabolomic profiling of mice serum during toxoplasmosis progression using liquid chromatography-mass spectrometry. *Sci Rep* 6:19557
- Zhou DH, Zhao FR, Huang SY, Xu MJ, Song HQ, Su C, Zhu XQ (2013) Changes in the proteomic profiles of mouse brain after infection with cyst-forming *Toxoplasma gondii*. *Parasit Vectors* 6:96

**Publisher's note** Springer Nature remains neutral with regard to jurisdictional claims in published maps and institutional affiliations.